PUB-77-140-E
E 416

E416
Phys. Rev.

VTL-PUB-38
(MAY 1977)
FERMILAB-PUB-77-140-E

"STUDY OF FINAL STATES IN $\pi^- N \to \mu^+\mu^-$ + HADRONS AT 225 GeV"*

A. M. JONCKHEERE,† V. COOK, S. CSORNA, D. HOLMGREN,
H. J. LUBATTI, P. MALECKI,†† K. MORIYASU, B. ROBINSON#

Department of Physics, University of Washington
Seattle, Washington 98195, USA

D. FOURNIER, P. HEUSSE, J. J. VEILLET

Laboratoire de l'Accélérateur Linéaire
91405 Orsay, France

J. H. KLEMS, W. KO, R. L. LANDER, D. E. PELLETT

Department of Physics, University of California
Davis, California 95616, USA

* Work supported in part by ERDA, NSF, and CNRS.

† Present address: Fermi National Accelerator Laboratory, Batavia, Illinois 60510.

†† Visitor from the Institute of Nuclear Physics and the Institute of Nuclear Physics and Technology of the Academy of Mining and Metallurgy, Krakow, Poland.

Present address: University of Pennsylvania, Philadelphia, Pennsylvania 19174.

ABSTRACT

An investigation is made of the final state hadrons produced in association with muons by a 225 GeV π^- beam interacting with a Lucite target. It is found that the hadrons produced in association with muon pairs do not differ significantly from hadrons produced in any other inelastic interaction. Cross sections for ψ/J production in Lucite and Pb and upper limits for charmed particle production are obtained. A comparison is made with models of ψ/J production.

I. INTRODUCTION

The study of lepton production in hadron-hadron interactions has led to unexpected observations: the presence of "anomalous" lepton production and the discovery of the ψ/J mesons. As yet, little or no information is available on the hadrons which are produced in association with the ψ/J meson. More recently, resonances which have been identified as charmed meson and baryon states have been observed in e^+e^- annihilation[1] and photo-production,[2] respectively. However, to date no conclusive evidence for charmed quantum number production in hadron-hadron interactions exists.

In this paper, we discuss the hadrons which are produced in association with prompt muons by interactions of 225 GeV negative pions in a Lucite ($C_5H_8O_2$) target. The hadrons are detected in the University of Washington's one-meter streamer chamber[3] which has good efficiency for detecting K_S^o's and Λ's which are backward in the CMS. The muons are defined by a magnetized iron absorber and their momenta measured in downstream wire spark chambers. We look for differences between interactions containing $\mu^+\mu^-$ pairs and those in which no μ selection is made. With a sensitivity of 22 dimuon events/nb, we find no significant differences in charge multiplicity, strange particle production (both numbers and momentum distribution), and rapidity distribution of the charged particles. Cross sections for ψ/J production on Lucite and Pb targets and upper limits for the production of charmed particles which decay semileptonically are obtained and compared with model predictions. Partial results have already been reported.[4]

In Sec. II, we describe the apparatus and give geometrical acceptances. The trigger cross sections are given and backgrounds discussed in Sec. III. The results and ψ/J cross sections are presented in Sec. IV. In Sec. V

an upper limit to charmed particle production is obtained.

II. APPARATUS

The apparatus used in the experiment, shown in Fig. 1, consists of three main sections: i) a beam-defining counter array, ii) the University of Washington streamer chamber, and iii) a muon spectrometer.

A 225 GeV mixed negative beam of 2 - 7 x 10^5 particles per 800 ms spill in the Fermilab M1 beam line was used. The beam species was tagged by two upstream threshold Cherenkov counters. A scintillator telescope array produced the logical beam signal (B); the beam halo was eliminated by veto counters located immediately upstream of the streamer chamber. Additional counters tagged those events with multiple beam particles or multiple interactions in the sensitive time of the streamer chamber.

The primary detector was the 1 x 0.5 x 0.3 m^3 streamer chamber with a 5.22 cm Lucite ($C_5H_8O_2$) target. The chamber was mounted inside a large momentum analyzing magnet, which provided a field of approximately 8 kG in the visible region of the chamber. The streamer chamber was viewed by three high-speed cameras from 2.5 meters at a maximum stereo angle of 15°. At the downstream end of the chamber was a large scintillation counter (S), with a 4.5 cm exit hole for non-interacting beam particles. A signal from this counter in coincidence with the beam signal defined an event: $E \equiv B \cdot S$.

Downstream of the streamer chamber was the muon spectrometer. This was composed of 5 meters (29 absorption lengths) of lead and iron absorber and eight muon telescopes. The first 40 cm of lead was placed inside the streamer chamber magnet, 150 cm from the target. A 10 cm square beam exit hole through this lead block was necessary to reduce spurious E triggers

due to backscatters. Outside of the magnet there was a solid 31 cm block of lead, followed by a 3 meter section of magnetized iron, the SOD magnet. This magnet, with 50 ± 6 kG-m of bending power, hardened the muon spectrum, and in conjunction with 6 planes of wire spark chambers downstream of the muon telescopes provided the sign of the charge and a measure of the muon momentum. Downstream of the muon telescope and spark chambers a calorimeter measured the hadron flux penetrating the muon filter.

The muon telescopes consisted of two planes of scintillation counters separated by 1.2 meters of iron. A muon trigger was defined by a coincident signal from corresponding counters in both planes. In the non-bend (horizontal) plane, the telescope accepted muons produced at angles from 9 to 94 mrad on either side of the beam; the maximum angle corresponds to approximately 90° in the πN center-of-mass system. Eliminating very forward angles reduced the trigger rate from beam muons and decreased the acceptance for forward muon pairs of very low invariant mass. In the bend (vertical) plane, the muon counters subtended 2 to 44 mrad on either side of the median plane.

The apparatus is most sensitive to forward muons and backward V°'s in the CMS. The 1μ and K_S^o efficiencies are given in Fig. 2 as a function of Feynman x_F and p_T. We note that for $p_T < 600$ MeV/c, the 1μ acceptance falls rapidly due to the 18 mrad gap in the muon counter array.

III. TRIGGER CROSS SECTIONS AND BACKGROUND

Various triggers were used, all of them requiring first a clean beam particle (B) defined by beam counters and veto hole counters which remove beam halo. An interaction (E) was defined as the coincidence between B and the S-counter (see Fig. 1) which is placed at the end of the streamer chamber. A one-muon event (1μ·E) was defined as the coincidence between an

interaction (E) and one of eight muon telescopes. Two muon events ($2\mu \cdot E$) required two different muon telescopes. Most of the data were taken with these triggers. However, in order to estimate the contribution of interactions in the absorber, data were also taken without the E requirements; i.e., a beam particle in coincidence with one muon telescope ($1\mu \cdot B$) or two muon telescopes ($2\mu \cdot B$). A comparison sample of E triggers was taken simultaneously with the $2\mu \cdot E$ triggers. The streamer chamber data were used to correct for systematic errors in the measured trigger rate, and these corrected rates are given in Table I. Table II gives the corresponding cross sections assuming atomic number dependence A^n for $n = 0.67$ and $n = 1$.

An analysis of 448 events in which a particle entered the calorimeter placed behind one of the muon telescopes gave no evidence of hadron signal. We thus conclude that the hadron punch-through contribution is negligible and that we were triggered by muons.

The question of whether these muons are prompt or the result of π and/or K decay in the streamer chamber or absorber is investigated by Monte Carlo techniques using data from 205 GeV $\pi^- p$ interactions in the Fermilab 30" bubble chamber.[5] Each track observed in the bubble chamber is propagated through the streamer chamber and the absorber. The probability that it decays or that one of the secondary particles produced by a hadronic cascade in the absorber decays is determined. We assume that 10% of the charged particles are kaons,[6] and that these kaons have the same momentum distribution as the pions. In the hadronic cascade, the number of secondaries at each stage is assumed to follow the usual Poisson distribution and the energy assumed to be equally divided among the secondaries.[7] The trigger rate due to decays in flight for each trigger configuration (Table I, Row 3) is obtained by weighting probabilities for each primary interaction multiplicity by the multiplicity distribution

observed in the E trigger. From these calculations, it is determined that:

i) The predicted dimuon trigger rate ($2\mu\cdot E$) from π and/or K decays is less than 7% of the observed rate;

ii) The predicted single muon trigger rate ($1\mu\cdot E$) is consistent with that observed.

An upper limit of the background due to π and K decays in the 2μ trigger can be estimated independently of the Monte Carlo, assuming that the $1\mu\cdot E$ rate is due entirely to decays. Then an upper limit for the dimuon trigger rate from decays is:

$$(2\mu\cdot E/E)_{decay} < 3/8\ (1\mu\cdot E/E)^2$$

The 3/8 results from a factor 1/2 to correct for double counting and 3/4 from our acceptance. From the rates in Table I, we conclude by this technique that less than 7% of the 2μ triggers could be due to π or K decays.

In addition, we shall see in Sec. IV that more than 90% of the reconstructed pairs are of unlike charge. This confirms that the contribution to our $2\mu\cdot E$ trigger from π and K decay is negligible.

It is necessary to determine for the $2\mu\cdot E$ events whether the muons are produced by primary interactions in the target or secondary interactions in the absorber. Using the spark chamber data, which gives a measurement of the muon position and direction after the magnetized absorber, an estimate of the production point can be made by a straight line backwards extrapolation in the non-bend plane. When both muons are reconstructed in the spark chambers, a common production point can be found; when only a single muon is reconstructed, the intersection with the beam plane is used. Errors on the position of the production point are largely due to multiple scattering in the absorber, so that the origin assignment cannot be made on an event-by-event basis. However, a statistical treatment gives comparable results when either one or

two muons are reconstructed and yields a best estimate of 55 ± 4% for the fraction of 2μ·E events which originate in the target.

We thus conclude that while the 1μ events are dominated by π and K decays, the 2μ events correspond to prompt muons with a decay background less than 7%, and 55 ± 4% are produced in the target by the primary interaction.

IV. RESULTS

In this section we discuss the dimuon mass spectrum obtained from interactions in Lucite (2μ·E) and lead (2μ·B) and present cross sections for ψ/J production. We also discuss in detail for the 2μ·E trigger the hadrons which are produced in association with dimuons.

A. Dimuon Mass Measurement

The dimuon mass spectrum is calculated from measurements of the momenta of the muons which produced the trigger. The momentum is obtained by swimming the track in the spark chambers through the magnetized iron and requiring it to intersect the Lucite target in the case of 2μ·E triggers, or to intersect the beam plane at a point one interaction length into the lead absorber in the case of the 2μ·B triggers. As was discussed in Sec. III, approximately half of the 2μ·E triggers in fact originate from interactions of the secondaries in the absorber. The 2μ·E events are fitted both with the muon origin in the Lucite target and one interaction length into the absorber. The final sample of 2μ·E dimuons used in the $M_{\mu^+\mu^-}$ plots contains only those events for which the χ^2, which was calculated assuming that the interaction occurs in the target, was smaller than that obtained assuming the interaction occurs in the absorber.

After making the appropriate χ^2 selections, we find 29 2μ·E events with muons of opposite sign reconstructing to the target out of 1148

triggers and 49 $2\mu\cdot B$ events with both muons reconstructing to the absorber out of 2808 triggers. In the same samples, we find three $2\mu\cdot E$ and two $2\mu\cdot B$ events where a muon pair of like charge satisfies the same reconstruction criteria. The efficiency for obtaining both muons in the spark chambers was low since the chambers did not cover the entire area of the muon telescopes and had intrinsically low two-track efficiency.

The dimuon mass spectra for interactions both in Lucite and in lead are shown in Fig. 3. The dashed curve shows the experimental acceptance as a function of mass for muon pairs, as determined by a Monte Carlo calculation. For the calculation, we assume the dimuon system is produced uniformly in Feynman x_F, $0 < x_F < 1$, with $d\sigma/dp_T^2 \propto \exp(-p_T^2)$, and decays isotropically in its rest frame.

Most of the events have low dimuon mass, between 0.2 and 1.8 GeV/c^2, similar to other dimuon production experiments.[8] Vector mesons cannot account for most of these events. An average of 0.35 ρ^o's per event has been observed in $\pi^- p$ interactions at 200 GeV.[9] Anderson et al.,[8] for pBe interactions at 150 GeV, observe approximately the same ρ production and, in addition, that $\sigma_\rho \simeq \sigma_\omega$. Therefore, assuming an average of 0.7 ρ^o's or ω's per event produced with $d\sigma/dx_F \propto (1-x_F)^{4.7}$ and $d\sigma/dp_T \propto p_T \exp(-3.8\, p_T)$,[10] we expect 4 ± 2 and 6 ± 3 ρ^o or ω mesons in the $2\mu\cdot E$ and $2\mu\cdot B$ samples, respectively.

The width of the ψ/J is consistent with our mass resolution, which is dominated by multiple Coulomb scattering of the muons in the 5 meters of absorber. We estimate a mass resolution of approximately $\pm$ 20% which is consistent with the data. We have 5 events for Lucite interactions and 9 events for lead interactions, respectively, in the region $2.6 \leq M_{\mu^+\mu^-} \leq 3.6$ GeV/c^2 which we identify with ψ/J production. Assuming a linear atomic number

dependence[11] of the cross section and correcting for all efficiencies and the acceptance,[12] we obtain:

$$B_{\mu\mu}\ \sigma_{\psi/J} = 15 \pm 7 \text{ nb/nucleon} \quad \text{- Lucite}$$

$$B_{\mu\mu}\ \sigma_{\psi/J} = 10 \pm 3 \text{ nb/nucleon} \quad \text{- Pb.}$$

These results agree well with the cross section $B_{\mu\mu}\ \sigma_{\psi/J} = 10.5 \pm 1.7$ nb/nucleon obtained by Anderson et al.[13] for $\pi^- C$ interactions at 225 GeV.

B. Correlations Between Hadrons and Muons

The streamer chamber photographs corresponding to the various triggers discussed in Sec. III were scanned for interactions in the target. For each interaction the number of minimum ionizing tracks, nuclear fragments and electrons from the target was listed as well as all neutral decays which pointed to the target. Any charged decays were also noted. The fast tracks from the target and the vertices and tracks of neutral decays (V^o's) were measured on an image plane digitizer. Approximately 60% of all pictures were scannable and contained a single interaction in the target. This result is essentially independent of trigger. The film was copied and has been scanned twice at each of the three collaborating institutions. The differences between the two scans were resolved by a physicist.

The V^o sample suffers losses from low detection efficiency near the interaction vertex because of confusion with the charged tracks, and can be contaminated by gammas which convert on the central wire plane.[14] Using pinhole optics, the vertex position has been reconstructed to ± 1 cm along the axes perpendicular to the streamer chamber. Identified gammas (neutral decays with both of the tracks having momentum less than 250 MeV/c yet minimum

ionizing) were used to verify that the electron-positron pairs originate on the central plane. From these studies, we concluded that the strange particle sample contains an appreciable gamma contamination (approximately 10%) which is localized along the central wire plane and thus can be deleted by a suitable fiducial cut about the central plane.

The distribution of the distance between the V^o vertex and the center of the target is not sensitive to reconstruction precision and is shown in Fig. 4. We note the non-exponential shape of Fig. 4a which exhibits the presence of the gamma contamination and detection inefficiency. The plot in Fig. 4b, which excludes the region within ± 1.5 cm of the central plane and 10 cm of the interaction vertex, shows no such effect. The straight line in Fig. 4b is an approximate fit to the data and corresponds to K_S^o with an average momentum of 5.6 GeV/c. We, therefore, conclude that we are able to isolate a good sample of V^o's free from gamma contamination with the above V^o fiducial volume.

The principal results obtained from the scan of the streamer chamber film for the E and 2μ·E triggers are tabulated in Table III. We list the number of events, average charge multiplicity $< N_{ch} >$, and dispersion $D \equiv (< N_{ch}^2 > - < N_{ch} >^2)^{\frac{1}{2}}$ for all events and those containing neutral decays. The average number of neutrals per event and the fraction of events containing neutral decays are also given. We also show the effect of the V^o fiducial volume cut which was described above. It should be noted that Table III shows no significant differences between the E and the 2μ·E samples.

A more detailed comparison of the 2μ·E and the E trigger is made in Figs. 5 to 7. Whenever appropriate, we also plot the data from 205 GeV $\pi^- d$ interactions obtained in an FNAL 30-inch bubble chamber experiment by the Davis-Krakow-Seattle-Warsaw collaboration (DKSW)[15] after making corrections for the streamer chamber

fiducial volume. Figures 5 and 6 give the charge multiplicity distributions for the full sample and for those events with neutral decays for both triggers. Figure 7 shows the average number of neutral decays as a function of the number of charged tracks in events with and without the V^o fiducial out.

The momentum distribution of the neutral strange particles was determined by measuring both tracks of the V^o and reconstructing their momenta. We determined the momentum of each track from the curvature in one view, choosing the view which had the best measurement. The assumption is that the magnetic field is perpendicular to the plane of the film in the view we choose. This introduces at most 10% error. We therefore obtain the momentum of the neutrals in that plane; since we know the V^o's direction in space from the vertex reconstruction, it is a simple matter to calculate the momentum of the V^o in space.

The V^o momentum distributions thus obtained are shown in Fig. 8 for the E and $2\mu \cdot E$ triggers. The distributions are the same for both triggers and, moreover, agree well with data obtained in $\pi^- d$ interactions at 200 GeV.[15] Figure 9 gives similar plots of the component of the V^o momentum transverse to the beam. The $2\mu \cdot E$ distribution is again in good agreement with the DKSW data. The E distribution appears to peak at lower momentum than the $2\mu \cdot E$, but the difference has only marginal statistical significance. Part of the skewing towards small p_T is due to the cut around the central plane (see A. Jonckheere, Ref. 4).

We have also measured the projected production angle of a sample of charged tracks for the E and $2\mu \cdot E$ triggers and calculated the rapidity $y_{pj} \simeq \ell n \tan(\theta_{pj}/2)$. The data are shown in Fig. 10. Again, no statistically significant differences are observed between the E and $2\mu \cdot E$ triggers.

Furthermore, there are no differences in the hadrons as a function of dimuon mass in those events for which we have reconstructed the dimuon mass and have streamer chamber data. No enhancement of V^o's is observed with the high mass dimuons (only one of the ψ/J events contains a V^o), whereas, one might have expected an enhancement due to decays of charmed states produced in association with the ψ/J by the production process $\pi N \rightarrow \psi\bar{C}CX$. The projected rapidity y_{pj}, Fig. 10, shows no differences between events with $M_{\mu^+\mu^-} < 2.0$ GeV/c^2 and those with $M_{\mu^+\mu^-} > 2.0$ GeV/c^2. The dependence of the charged multiplicity on the dimuon mass (See Fig. 11) is consistent with being flat; however, we cannot exclude a slight linear dependence of $< N_{ch} >$ on $M_{\mu^+\mu^-}$.

The effective mass of the muon and neutral strange particle is plotted in Fig. 12. To estimate background, we combine a muon and a V^o from different events taking $m_{V^o} = m_{K^o}$, and assume the effective mass distribution obtained is representative of the true phase space. We note a slight enhancement at $\sim$ 4 GeV which has marginal statistical significance, as it is only two standard deviations above the background.

We are led to conclude that the hadrons which are produced in association with muon pairs show no significant differences from those produced in any other inelastic interaction. The hadrons have the same charged multiplicity distributions and rapidity distributions; the neutral strange particles are distributed in the same way among the topologies and have similar momentum distributions. This is a somewhat surprising result since one might naively have expected some difference to be exhibited in these gross features if only because the dimuon cross section is such a tiny fraction (4×10^{-6}) of the total.

V. UPPER LIMIT ON CHARM PARTICLE PRODUCTION

From the lack of observed muon, strange-particle correlations noted above, an upper-limit on the charmed particle signal present in the data can be calculated.

Neutral strange particles with either the E or the $2\mu \cdot E$ trigger can be:

i) correlated with muons; i.e., charm decay, producing an average number of strange particles per event: $\langle V^o \rangle_c$

ii) or, uncorrelated with muons; i.e., normal strange particle production, producing: $\langle V^o \rangle_s$.

But, since the E trigger V^o production should be dominated by "normal" production, we can isolate the muon-correlated (charm) signal in the $2\mu \cdot E$ data sample:

$$\langle V^o \rangle_c = \langle V^o \rangle_{2\mu} - \langle V^o \rangle_E .$$

This equation depends on three assumptions:

i) the contribution to strange particle production from charm is negligible in the total cross section;

ii) charm production and normal strange particle production are independent and nonexclusive; and

iii) normal strange particle production is independent of muon production.

From Table III we find $< V^o >_c = 0.003 \pm 0.0132$ muon correlated strange particles per event. This result is not sensitive to the various cuts we have applied to the data. This number easily can be converted to a cross section upper limit at the 90% confidence level:

$$\sigma_{obs} \leq (< V_o >_c + 1.28\ \delta_c)\ \sigma_{2\mu \cdot E} = 0.57 \text{ nb.}$$

Here δ_c is the statistical error, $\sigma_{2\mu \cdot E}$ is the trigger cross section from Table II, and the factor 1.28 is the 90% confidence limit for a normal distribution with unit deviation; we have assumed the charm cross section has a linear atomic number dependence. This is a model independent limit on the charm signal present within the acceptance of this apparatus.[16]

In order to remove the acceptance from this limit, we must resort to models for the production and decay of charmed states. For production of $D\bar{D}$ pairs with $M_D = 1.87$ GeV/c^2, we assume that the dominant D decay modes which produce muons in the final state are leptonic ($D \to \mu\nu$) and semi-leptonic ($D \to K^*_{890}\mu\nu$).[17] Because we take as our charm signal two muons and a neutral strange particle, we are sensitive to two final states:

1) Both D's decay semileptonically;

2) One decays semileptonically, the other leptonically.

Let g_1 and g_2 be the corresponding probabilities to observe a V^o with a 2μ trigger. These factors include the probability that the K^* produces a $K^o_S \to \pi^+\pi^-$ as well as the geometrical acceptance of the apparatus. Then the observed cross section is:

$$\sigma_{obs} \geq \sigma_{D\bar{D}}\ (B_{SL}{}^2 g_1 + 2B_{SL}B_L g_2),$$

where B_{SL} and B_L are the semileptonic and leptonic branching ratios,

respectively, and $\sigma_{D\bar{D}}$ the production cross section for the $D\bar{D}$ pair.

Acceptances were determined by Monte-Carlo methods for two production models:[18]

i) each D was produced with the momentum distribution observed for ψ/J production cited above and

ii) the $D\bar{D}$ pair was produced diffractively with an exp(10t) distribution and internal kinetic energy Q = 400 MeV.

For either model, each D then decayed isotropically in its rest frame; the muons were propagated through the apparatus taking multiple scattering and energy loss into account. The probability that both muons and at least one K_S^o would have been observed was determined. We obtain $g_1 = 2.6 \times 10^{-3}$ and $g_2 = 2.1 \times 10^{-3}$ for the ψ/J production mechanism and $g_1 = 5.4 \times 10^{-3}$ and $g_1 = 3.2 \times 10^{-3}$ for the diffractive mechanism. If we assume $B_{SL} = B_L = B$ then our limit becomes $\sigma^{obs} \geq \sigma_{D\bar{D}} B^2 g$, where $g \equiv g_1 + 2g_2$. Further, assuming that B = 0.1, we obtain $D\bar{D}$ limits of

$$\sigma_{D\bar{D}} < 8.5 \text{ ub for } \psi/J\text{-like production}$$

$$\sigma_{D\bar{D}} < 4.8 \ \mu\text{b for diffractive production}$$

V. CONCLUSION

We have measured the cross section for hadronic production of ψ/J mesons, and have found our results to be in good agreement with those of Ref. 13. Only a small fraction ($\sim$ 15%) of the low-mass dimuons can be accounted for by vector meson production.[19] At the level of 22 events/nb we find that the hadrons produced with muon pairs are the same as hadrons produced in any inelastic interaction. The absence of correlated μ-V^o production leads to an upper limit on the cross section for production of new states which decay semi-leptonically. Choosing two specific models for production of $D\bar{D}$ charmed

mesons with $m_D = 1.87\ GeV/c^2$ and using a 10% semileptonic and leptonic branching ratio we calculate an upper limit for the production cross section of $\sigma_{D\bar{D}} \leq 8.5\ \mu b$ for the ψ/J production model of $\sigma_{D\bar{D}} \leq 4.8\ \mu b$ for the diffractive production model.

The cross sections obtained above may be used to compare with models of hadronic production of ψ/J mesons. Using our cross section for ψ/J production in Lucite $B_{\mu\mu}\sigma_{\psi/J} = 15 \pm 7$ nb and the branching ratio $\Gamma_{\psi \to \mu\mu} = 0.07$, we obtain $\sigma_{\psi/J} = 0.22 \pm 0.10\ \mu b$.

Comparing the upper limit of the cross section for $D\bar{D}$ production to $\sigma_{\psi/J}$, we find

$$\sigma_{D\bar{D}}/\sigma_{\psi/J} \leq 22 \quad \text{Diffractive model}$$

$$\sigma_{D\bar{D}}/\sigma_{\psi/J} \leq 39 \quad \psi/J \text{ model}$$

These upper limits can be used to obtain information on the production mechanism of the ψ/J mesons. It has already been demonstrated by comparing the upper limits for $\sigma_{D\bar{D}\ \psi/J}/\sigma_{\psi/J}$ that the Okubo-Zweig-Iizuka (OZI) mechanism cannot account for more than 1% of the hadronic production of ψ/J's[20] at Fermilab energies. Our results are consistent with the conclusion that the OZI mechanism is not important since Sivers[21] obtains $\sigma_{D\bar{D}}/\sigma_{\psi/J} \simeq 650$ which is 15 to 30 times larger than the limits obtained above.

An alternate mechanism for the observed ψ/J production has been proposed by Ellis et al.[22] They propose that the ψ/J observed in hadronic interactions result dominantly from production of $C = +1$ $c\bar{c}$ states which subsequently decay to γ (or hadrons) + ψ/J.

We have used the form of the differential cross section $d\sigma_{c\bar{c}}/dm^2$ based on two gluon amalgamation given in Ref. 23 and calculated[24]

$$\sigma_{D\bar{D}}/\sigma_{\psi/J} \approx 24 \pm 4$$

Thus, our upper limits do not exclude the $c\bar{c}$ cascade model of ψ/J production; it would clearly be desirable to increase the statistics if this model is correct since our experiment was very close to observing $D\bar{D}$ production.

ACKNOWLEDGMENTS

We wish to thank R.R. Wilson for making the SOD magnet possible, P. Koehler and the staff of the Meson Laboratory at FNAL for assistance and encouragement, and the scanning staffs of our respective collaborators for their careful work. We are indebted to D. Forbush, K. Hayes, R. Kass, R. Kenyon, M. Maher, P. Rançon, D. Rosner, D. Reid, J. Schultz, F. Toevs, W. Wallick, and G. Wurden for technical assistance. We especially acknowledge the assistance of F. Rohrbach in the construction of the streamer chamber. We are grateful to S. Ellis for illuminating discussions concerning ψ/J production mechanisms.

REFERENCES:

1. I. Peruzzi et al., Phys. Rev. Letters 37, 569 (1976).

2. B. Knapp et al., Phys. Rev. Letters 37, 882 (1976).

3. V. Cook et al., Proc. Intern. Conf. on Instrumentation for high energy physics, ed. S. Stipcich (Laboratori Nazionali del CNEN, Servizio Documentazione, Frascati) 171 (1973).

4. V. Cook et al., Phys. Lett. 64B, 221 (1976); A. Jonckheere, "Streamer Chamber Search for New States of Matter which Decay Semileptonically", Ph.D. Thesis, University of Washington VTL-PUB-34 (1976).

5. D. Bogert et al., Phys. Rev. Letters 31, 1271 (1973).

6. L. Foá, J. Phys. (Paris) C1, 317 (1973).

7. Since it turns out that fewer than 20% of decay muons result from particles produced in the cascade in the absorber, the Monte Carlo is relatively insensitive to the equipartition of energy assumption.

8. K.J. Andersom et al., Phys. Rev. Letters 37, 799 (1976).

9. P.D. Higgins et al., "Inclusive ρ^o (75) and Δ^{++}(1236) Production in 200 GeV/c $\pi^- p$ Reactions", Bull. Am. Phys. Soc. 21, 544 (1976).

10. K.J. Anderson et al., Phys. Rev. Letters 37, 803 (1976).

11. The A dependence was predicted by J. Pumplin and E. Yen, Phys. Rev. 110, 812 (1975), and has been observed for dimuon mass $M_{\mu\mu} > 1$ GeV/c^2; see Binkley et al., Phys. Rev. Letters 37, 571 (1976) and Ref. 13.

12. The acceptance calculation uses the following distribution obtained from the data given by Anderson et al. (Ref. 13),

$$d\sigma/dx_F \propto \begin{cases} \text{const.} & 0 < x_F \leq 0.5 \\ \exp(-14.5\, x_F) & 0.5 \leq x_F < 1 \end{cases}$$

$$d\sigma/dp_T^2 \propto \exp\,(-0.6 p_T^2).$$

13. K.J. Anderson et al., "Production of the J(3.1) and ψ'(3.7) by 225 GeV π^+, π^- and Protons", submitted to XVIII Conference in High-Energy Physics, Tbilisi, USSR (1976).

14. Since the streamer chamber is gas filled, gammas have a negligible probability of converting except in the wires of the central high-voltage plane.

15. S. Csorna et al., "Inclusive Neutral Particle Production in π^-d Interactions at 205 GeV", University of Washington VTL-PUB-35 (1977). To be published in Nucl. Phys.

16. Using the number of events with V^o instead of the mean number of V^o per event gives a similar limit (σ_{obs} < 0.58 nb).

17. Private communication, DASP collaboration.

18. D. Holmgren, "Determination of E-416 Acceptances by Monte Carlo", University of Washington Internal Note VTL-HEP-40 (1977).

19. A. similar conclusion has been reached by H. Kasha et al., Phys. Rev. Letters 36, 1007 (1976).

20. J.G. Branson et al., Phys. Rev. Letters 38, 580 (1977) and M. Binkley et al., Phys. Rev. Letters 37, 578 (1976).

21. D. Sivers, Nucl. Phys. B106, 95 (1976).

22. S.D. Ellis et al., Phys. Rev. Letters 36, 1263 (1976).

23. M.B. Einhorn and S.D. Ellis, Phys. Rev. D12, 2007 (1975).

24. The calculation is based on the following assumptions:

i) color singlet $c\bar{c}$ states with mass between that of χ(3410) and that of two D mesons (3.74 GeV) will cascade down to the ψ/J (3100);

ii) $c\bar{c}$ states (not required to be color singlets) with mass between 3.74 and 7.07 GeV will cascade down to a $D\bar{D}$ pair.

TABLE CAPTIONS:

TABLE I : Trigger rates - errors quoted are statistical only. If no error is quoted, the error is less than the last significant digit.

TABLE II : Trigger cross sections; σ_n is the cross section per nucleon for an A^n atomic number dependence.

TABLE III : Scan results.

	E/B	1μ·E/B	2μ·E/B	1μ·E/E	2μ·E/E	1μ·B/B	2μ·B/B
Trigger Rate	$3.57 \pm .09 \times 10^{-2}$	$2.97 \pm .25 \times 10^{-5}$	$1.31 \pm .06 \times 10^{-7}$	$8.3 \pm .7 \times 10^{-4}$	$3.6 \pm .2 \times 10^{-6}$	3.9×10^{-4}	7.55×10^{-6}
Efficiencies	$.79 \pm .02$	$.85 \pm .07$	$.70 \pm .03$	$1.09 \pm .01$	$.88 \pm .05$	.93	.93
Monte Carlo				6.6×10^{-4}	0.24×10^{-6}		

TABLE I

TRIGGER	σ_n	
	n = 0.67	n = 1.0
E(mb)	19.6	9.2
1μ·E(μb)	16.3	7.6
2μ·E(nb)	70.5	33.1
3μ·E(nb)	4.1	1.9
2μ·E(nb) corrected for muon origin	38.8	18.2

TABLE II

TRIGGER	EVENTS	$\langle N_{ch} \rangle$	D	EVENTS W/V^o	$\langle N_{ch} \rangle_v$	D_v	# of V^o	$\langle V^o \rangle$
E	1908	12.4 ± .3	6.1 ± .3	269	13.0 ± .9	6.1 ± .7	300	.1572 ± .0093
		(with V^o cuts)[a]		161	13.0 ± 1.1	6.2 ± .9	172	.0901 ± .0070
2μ·E	719	12.7 ± .5	6.5 ± .4	98	13.6 ± 1.5	6.9 ± 1.1	103	.1433 ± .0138
		(with V^o cuts)[a]		62	13.7 ± 2.0	7.2 ± 1.3	65	.0904 ± .0112

[a] V^o cuts: Exclude ± 1.5 cm around central wire plane and 10 cm around primary vertex (see text).

TABLE III

FIGURE CAPTIONS:

FIG. 1 : Apparatus (a) Plan view of apparatus. (b) Muon telescope layout

FIG. 2 : The detection efficiency for (a) Muons and (b) K_S^o as a function of x_F and p_T.

FIG. 3 : Dimuon mass spectra.

FIG. 4 : Decay distance of neutrals (a) No cuts on data. (b) Deleting decays within 10 cm of the primary vertex and ± 1.5 cm of the HV wire plane.

FIG. 5 : Charged multiplicity - no cuts.

FIG. 6 : Charged multiplicity with one or more neutral decays - no cuts.

FIG. 7 : Average number of neutral strange decays observed versus number of charged tracks. (a) No data cuts. (b) Deleting decays within 10 cm of the primary vertex and ± 1.5 cm of the high-voltage wire plane.

FIG. 8 : Neutral strange particle laboratory momentum with V^o vertex position cuts.

FIG. 9 : Neutral strange particle transverse momentum with V^o vertex position cuts.

FIG. 10 : Projected rapidity.

FIG. 11 : Average charge multiplicity as a function of dimuon mass.

FIG. 12 : Muon-strange particle effective mass.

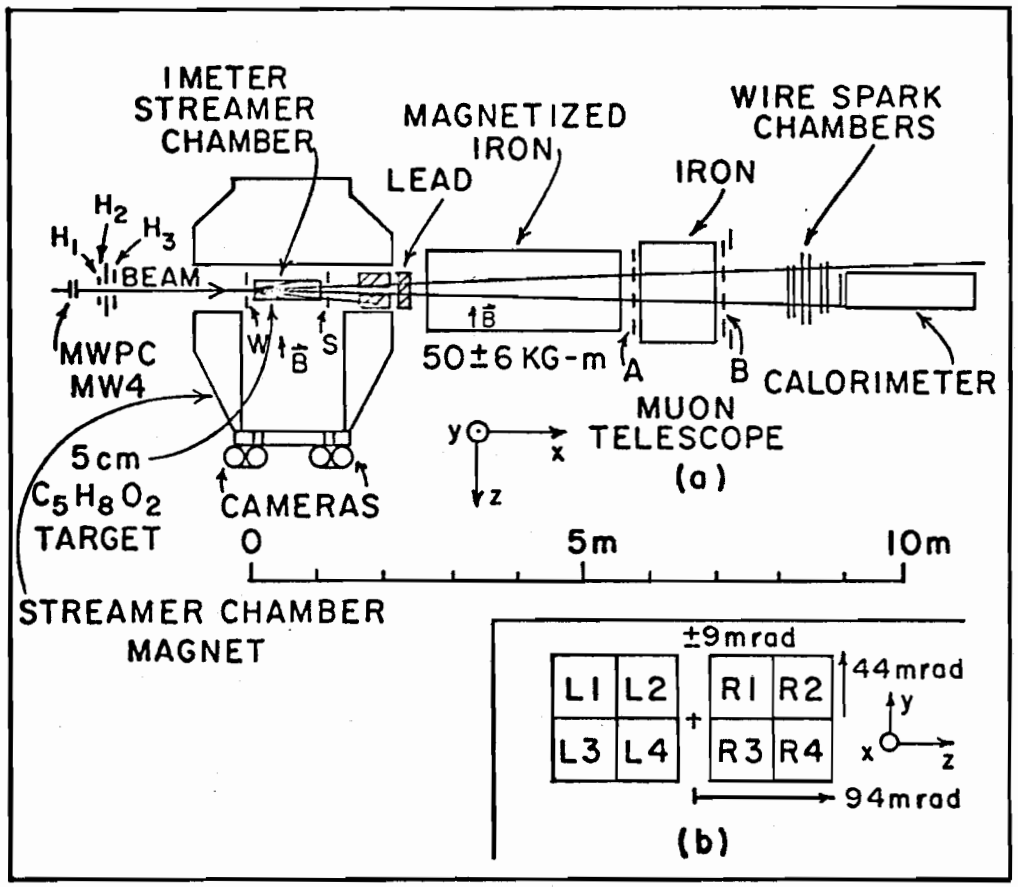
IMETER
STREAMER
CHAMBER
MAGNETIZED
IRON
WIRE SPARK
CHAMBERS
LEAD
IRON
H2
H1
H3
BEAM
MWPC
MW4
W
B
S
B
50±6 KG-m
A
B
CALORIMETER
MUON
TELESCOPE
(a)
y
x
z
5cm
C5H8O2
TARGET
CAMERAS
0
5m
10m
STREAMER CHAMBER
MAGNET
±9mrad
L1
L2
R1
R2
L3
L4
R3
R4
44mrad
y
x
z
94mrad
(b)

FIG. 1

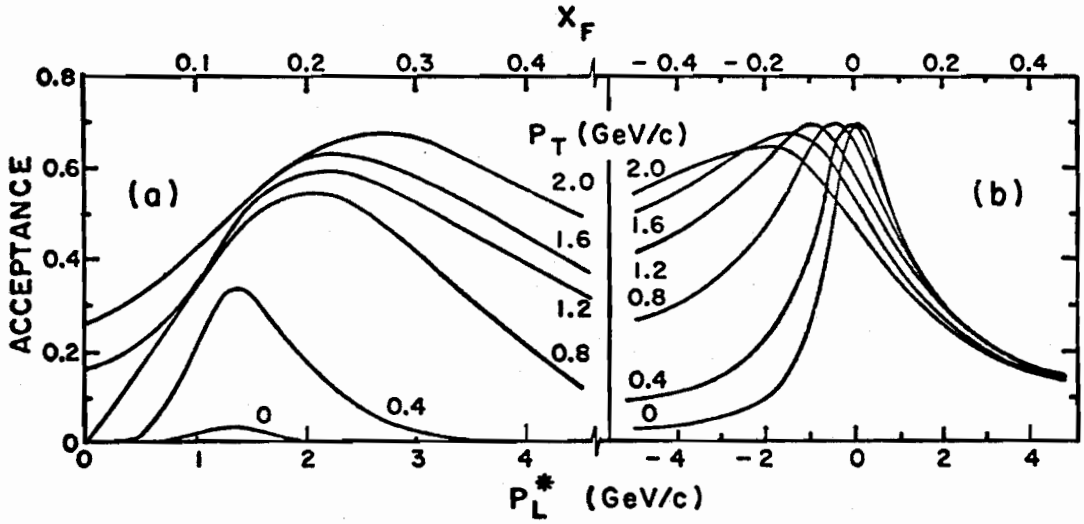
X_F
0.1
0.2
0.3
0.4
- 0.4
- 0.2
0
0.2
0.4
0.8
0.6
0.4
0.2
0
ACCEPTANCE
(a)
(b)
P_T (GeV/c)
2.0
1.6
1.2
0.8
0.4
0
0
1
2
3
4
- 4
- 2
0
2
4
P_L^* (GeV/c)

FIG. 2

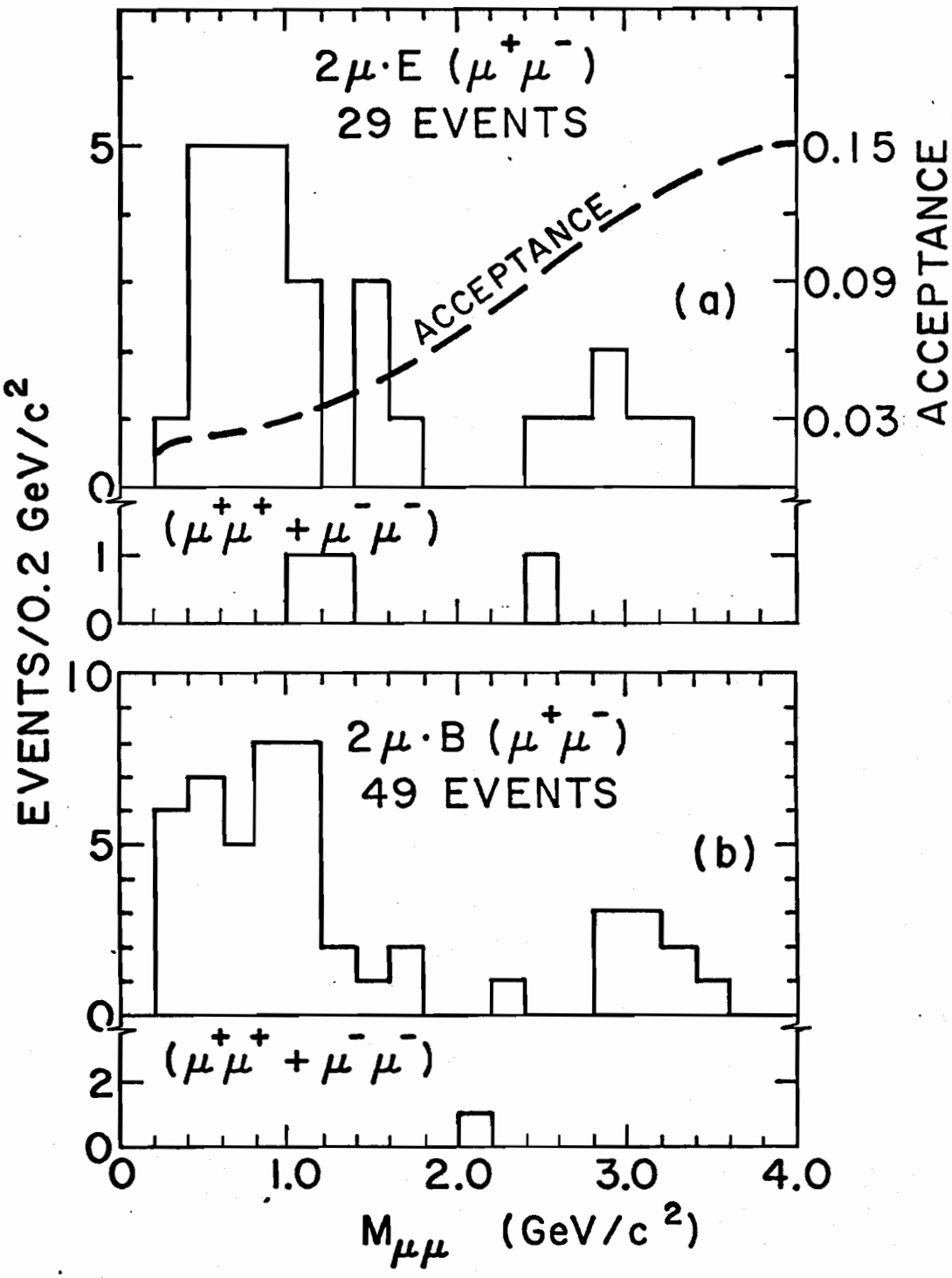
2μ·E (μ⁺μ⁻)
29 EVENTS
ACCEPTANCE
(a)
(μ⁺μ⁺ + μ⁻μ⁻)
2μ·B (μ⁺μ⁻)
49 EVENTS
(b)
(μ⁺μ⁺ + μ⁻μ⁻)
EVENTS/0.2 GeV/c²
ACCEPTANCE
0.15
0.09
0.03
5
0
1
0
10
5
0
2
0
0
1.0
2.0
3.0
4.0
M_μμ (GeV/c²)

FIG. 3

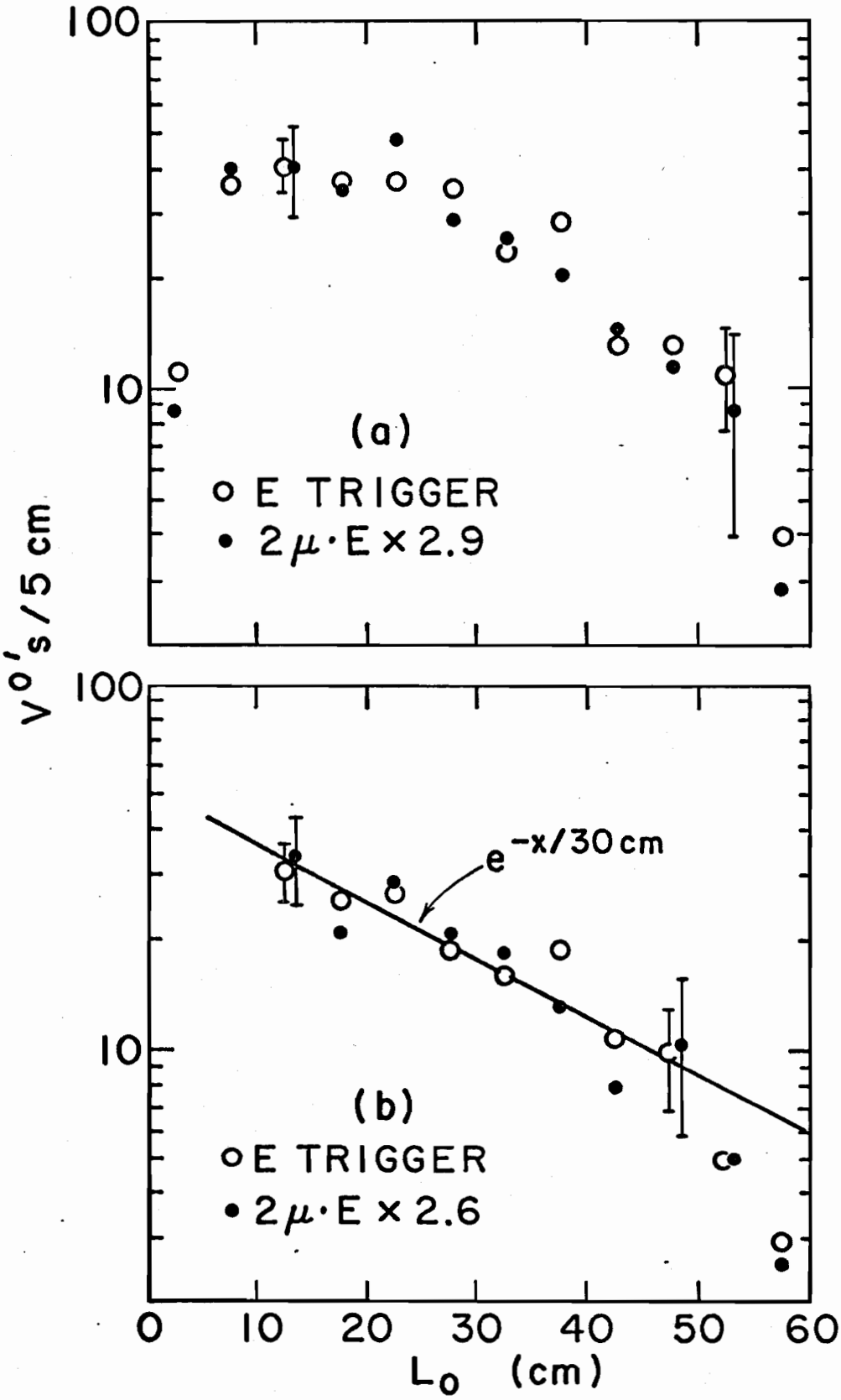
100
10
(a)
○ E TRIGGER
• 2μ·E × 2.9
V⁰'s/5 cm
100
10
e^-x/30 cm
(b)
○ E TRIGGER
• 2μ·E × 2.6
0
10
20
30
40
50
60
L₀ (cm)

FIG. 4

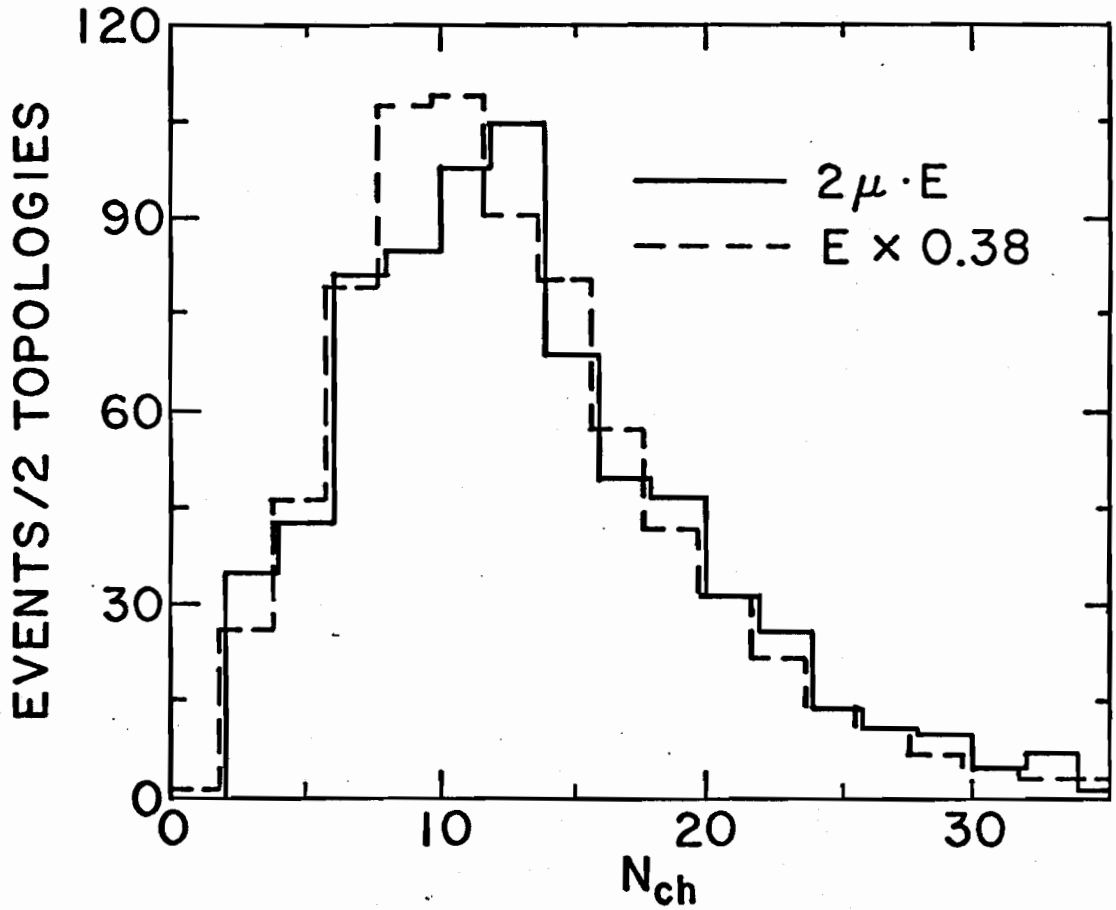
120
90
60
30
0
EVENTS/2 TOPOLOGIES
0
10
20
30
N_{ch}
$2\mu \cdot E$
$E \times 0.38$

FIG. 5

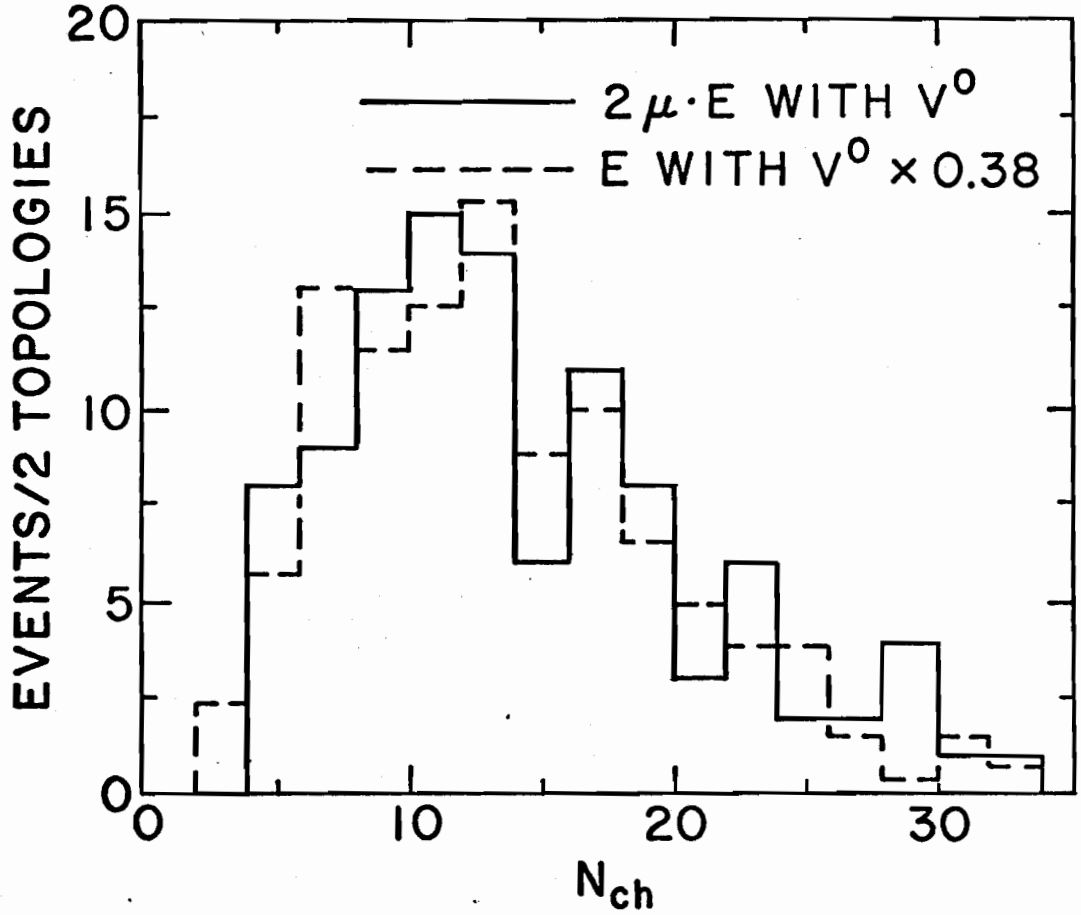
20
15
10
5
0
EVENTS/2 TOPOLOGIES
2μ·E WITH V⁰
E WITH V⁰ × 0.38
0
10
20
30
N_ch

FIG. 6

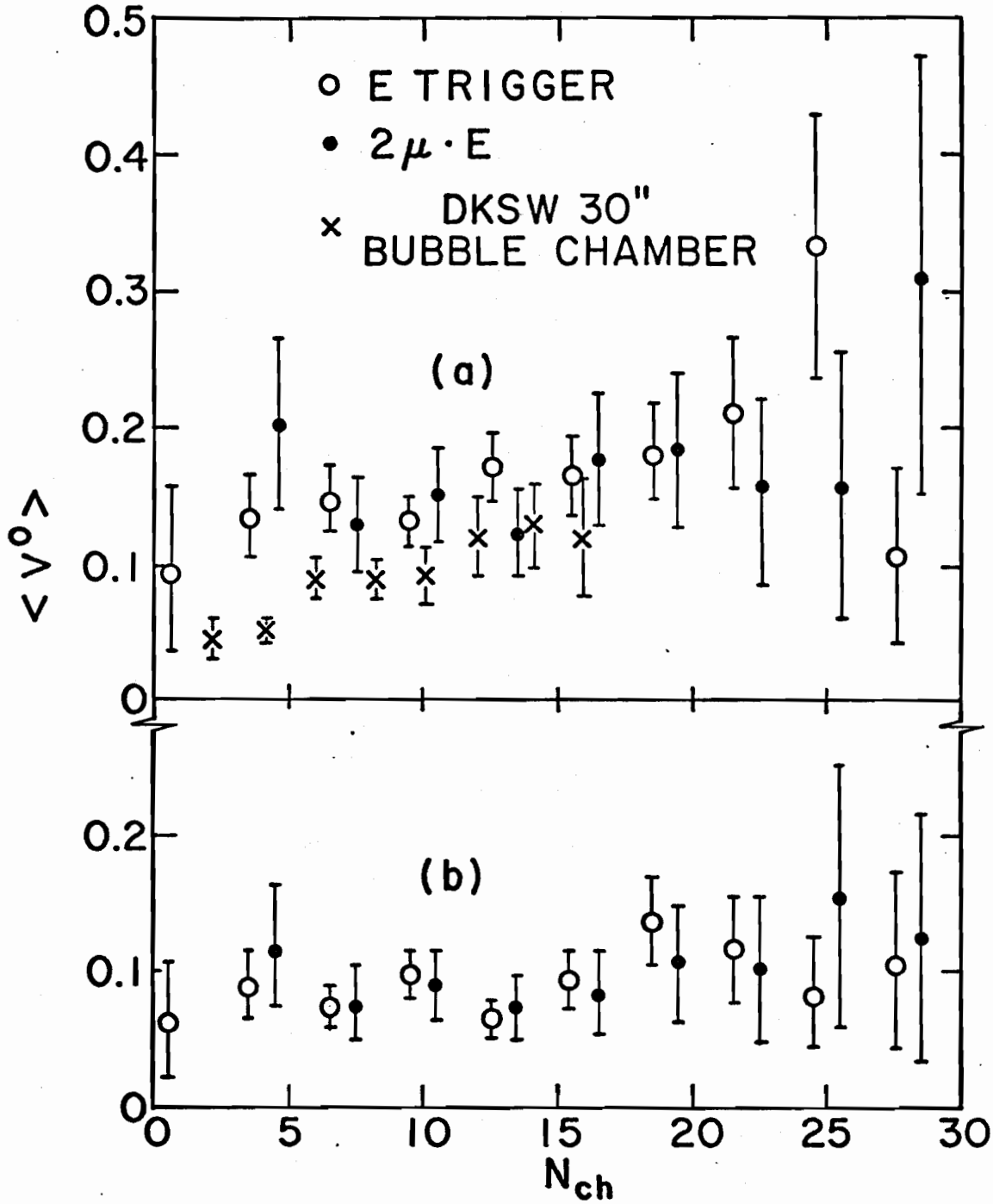
0.5
0.4
0.3
0.2
0.1
0
E TRIGGER
2μ·E
DKSW 30"
BUBBLE CHAMBER
(a)
(b)
<V°>
0
5
10
15
20
25
30
N_ch

FIG. 7

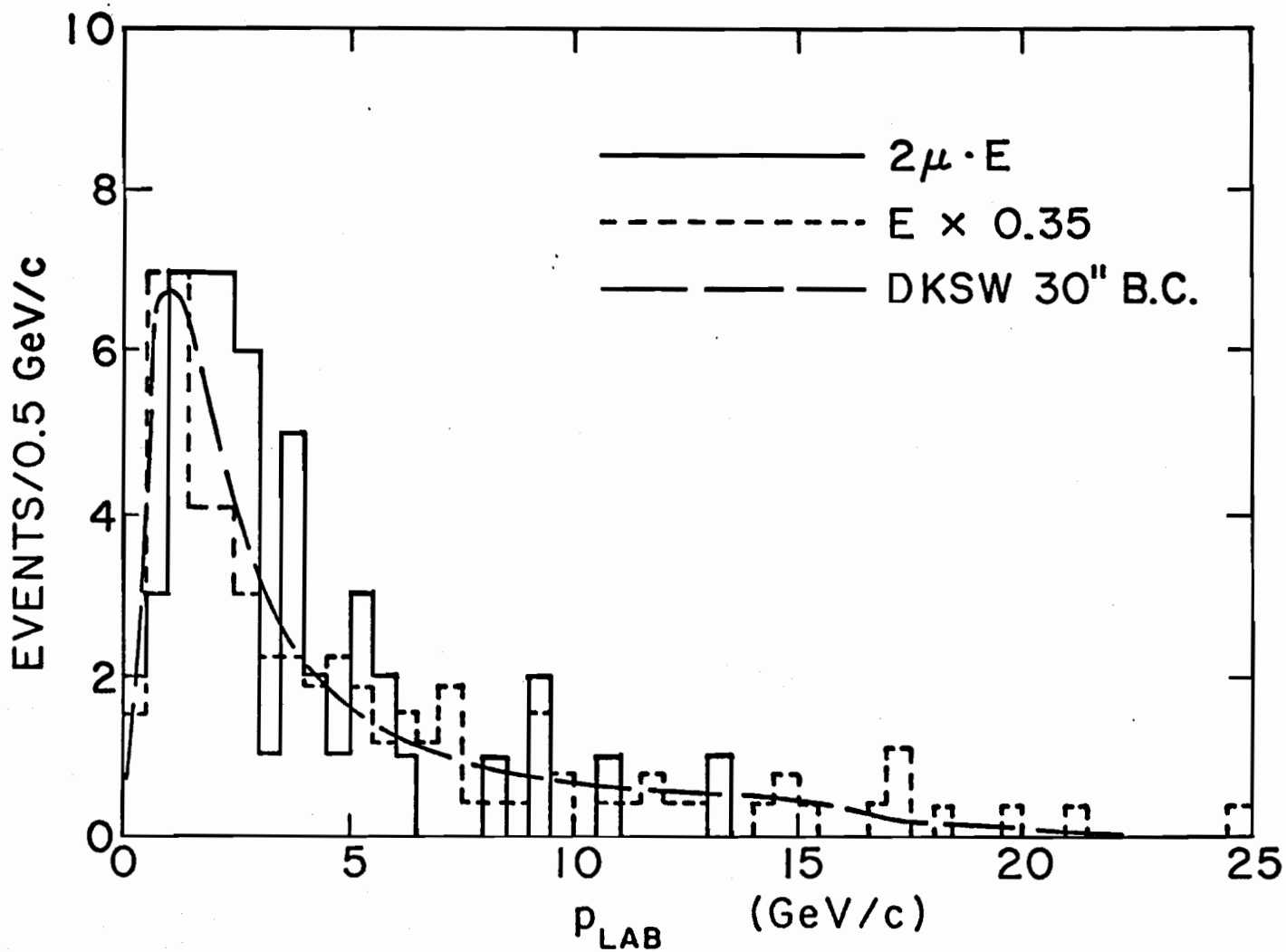
EVENTS/0.5 GeV/c
10
8
6
4
2
0
0
5
10
15
20
25
p_{LAB} (GeV/c)
$2\mu \cdot E$
E × 0.35
DKSW 30" B.C.

FIG. 8

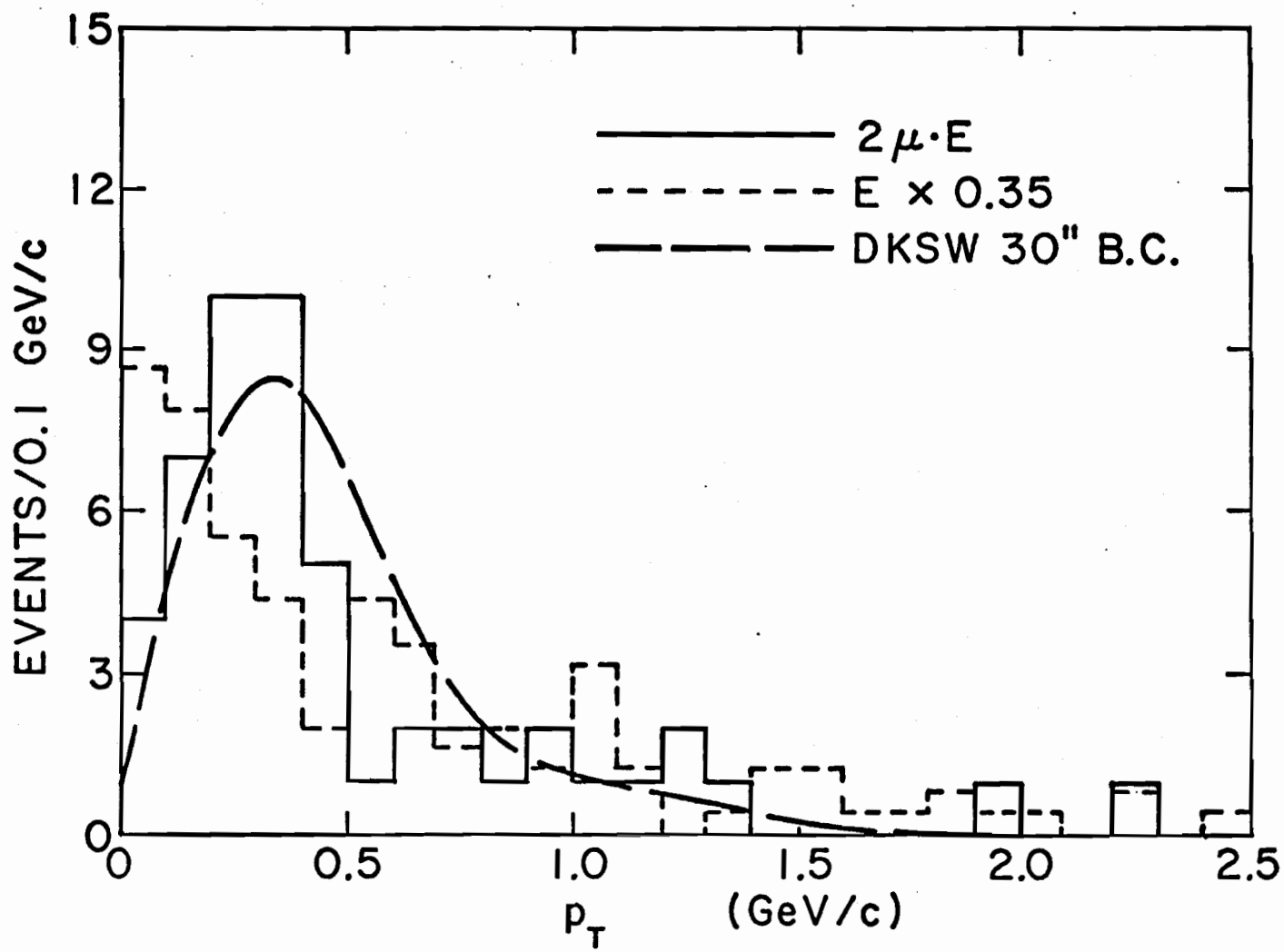
15
12
9
6
3
0
EVENTS/0.1 GeV/c
0
0.5
1.0
1.5
2.0
2.5
p_T (GeV/c)
2μ·E
E × 0.35
DKSW 30" B.C.

FIG. 9

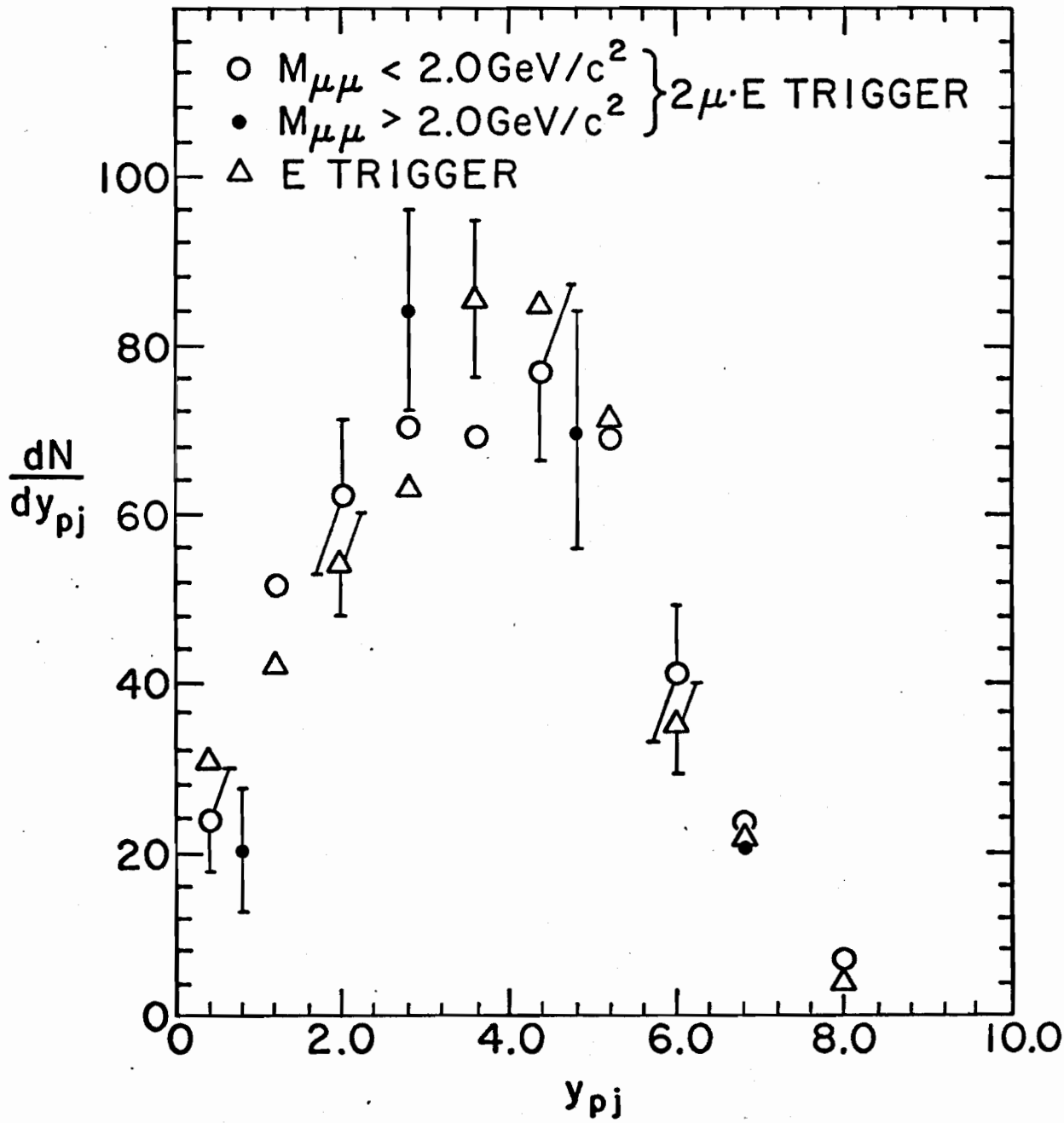
○ $M_{\mu\mu} < 2.0 GeV/c^2$
● $M_{\mu\mu} > 2.0 GeV/c^2$
} $2\mu \cdot E$ TRIGGER
△ E TRIGGER
$\frac{dN}{dy_{pj}}$
y_{pj}
0
20
40
60
80
100
2.0
4.0
6.0
8.0
10.0

FIG. 10

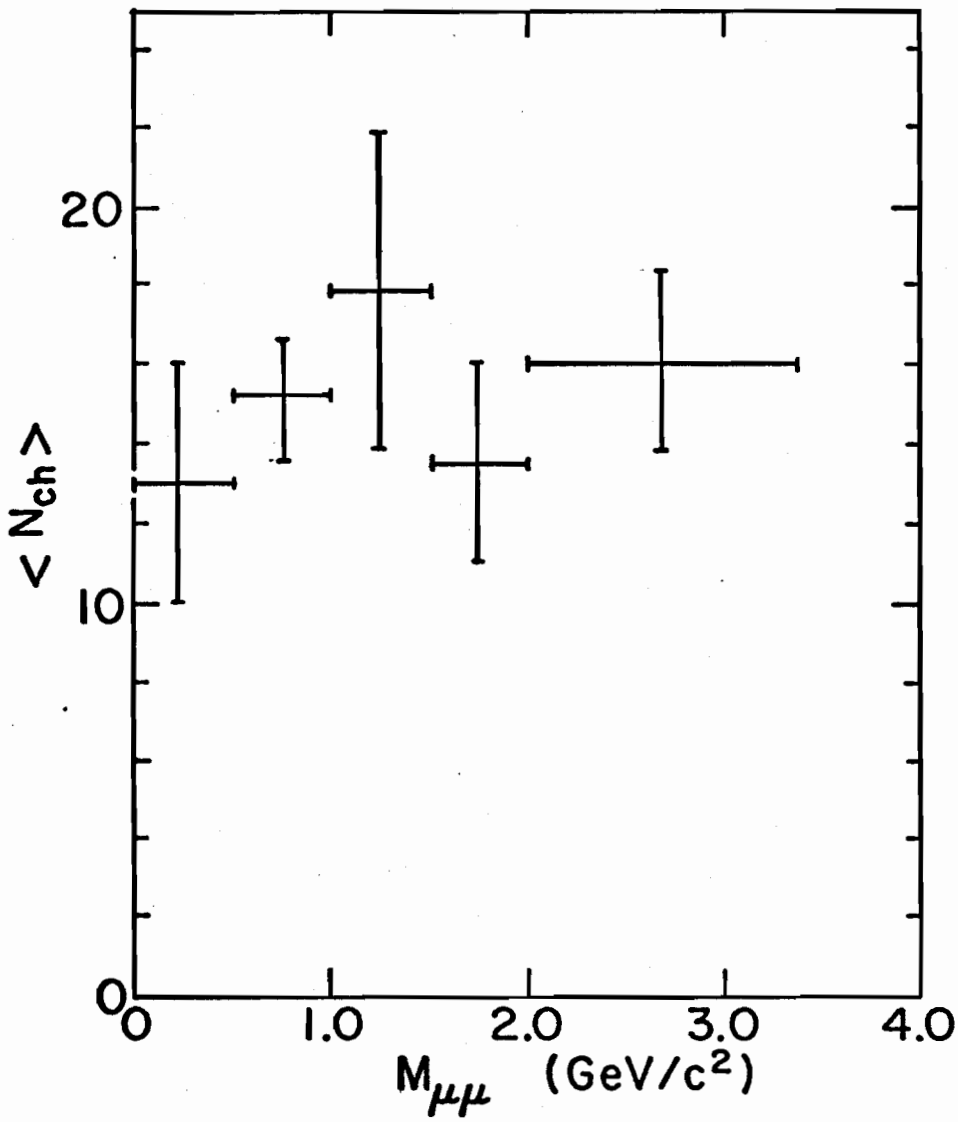

FIG. 11

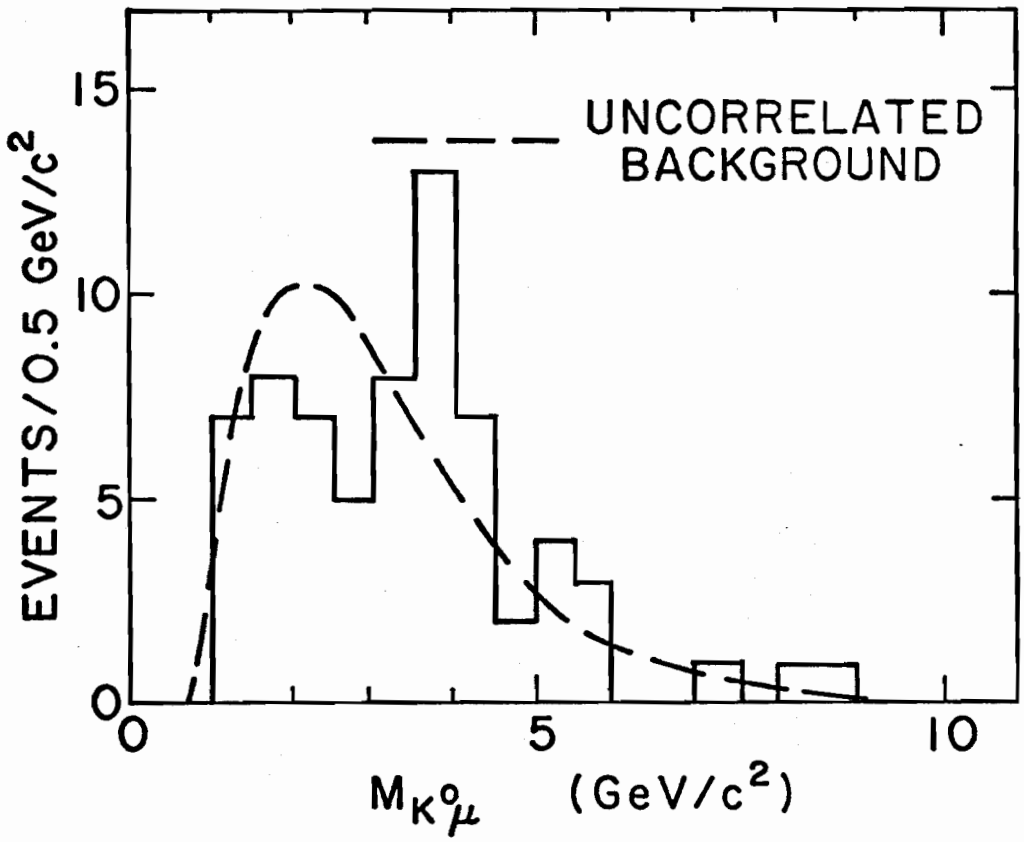
UNCORRELATED
BACKGROUND
EVENTS/0.5 GeV/c²
15
10
5
0
0
5
10
$M_{K^0\mu}$ (GeV/c²)

FIG. 12